NASA TECHNICAL NOTE

NASA TN D-5536

NASA TN D-5536

ANALYTICAL AND EXPERIMENTAL INVESTIGATION OF END-PLANE ROTATIONS OF TRUNCATED CONES UNDER BENDING LOADS

by Richard W. Faison, John L. Gilbert, and William H. Richards

Langley Research Center
Langley Station, Hampton, Va.

NATIONAL AERONAUTICS AND SPACE ADMINISTRATION • WASHINGTON, D. C. • NOVEMBER 1969

1. Report No. NASA TN D-5536	2. Government Accession No.	3. Recipient's Catalog No.
4. Title and Subtitle ANALYTICAL AND EXPERIMENTAL INVESTIGATION OF END-PLANE ROTATIONS OF TRUNCATED CONES UNDER BENDING LOADS		5. Report Date November 1969 6. Performing Organization Code
7. Author(s) Richard W. Faison, John L. Gilbert, and William H. Richards		8. Performing Organization Report No. L-6019 10. Work Unit No. 124-08-13-05-23
9. Performing Organization Name and Address NASA Langley Research Center Hampton, Va. 23365		11. Contract or Grant No. 13. Type of Report and Period Covered Technical Note
12. Sponsoring Agency Name and Address National Aeronautics and Space Administration Washington, D.C. 20546		14. Sponsoring Agency Code

15. Supplementary Notes

16. Abstract

Many engineering problems involving beam-type deflections are treated as elementary beams, and thus the stiffness parameter EI is of major significance in determining the proper deflections. When sections of the beam consist of thin-wall truncated cones, the parameter EI is not an adequate measure of the beam stiffness since shell behavior predominates. A correction coefficient which accounts for the degeneration of stiffness from that computed by use of elementary beam theory is presented to be applied to the stiffness parameter of thin-wall truncated-cone sections. The correction coefficient was determined by membrane-theory analysis of a truncated cone subjected to end-plane rotations, and corroborative experimental results were obtained from small-scale tests.

17. Key Words Suggested by Author(s)	18. Distribution Statement
Truncated cones End-plane rotations	Unclassified – Unlimited

19. Security Classif. (of this report)	20. Security Classif. (of this page)	21. No. of Pages	22. Price*
Unclassified	Unclassified	29	$3.00

*For sale by the Clearinghouse for Federal Scientific and Technical Information
Springfield, Virginia 22151

ANALYTICAL AND EXPERIMENTAL INVESTIGATION OF END-PLANE ROTATIONS OF TRUNCATED CONES UNDER BENDING LOADS

By Richard W. Faison, John L. Gilbert,
and William H. Richards
Langley Research Center

SUMMARY

Many engineering problems involving beam-type deflections are treated as elementary beams, and thus the stiffness parameter EI is of major significance in determining the proper deflections. When sections of the beam consist of thin-wall truncated cones, the parameter EI is not an adequate measure of the beam stiffness since shell behavior predominates. A correction coefficient which accounts for the degeneration of stiffness from that computed by use of elementary beam theory is presented to be applied to the stiffness parameter of thin-wall truncated-cone sections. The correction coefficient was determined by membrane-theory analysis of a truncated cone subjected to end-plane rotations, and corroborative experimental results were obtained from small-scale tests.

INTRODUCTION

In many engineering applications, problems involving elementary beam deflections are encountered. In such cases, the distribution of the stiffness parameter EI along the length of the beam is of major significance in performing the calculations. However, when sections of the beam consist of thin-wall truncated cones, the parameter EI is not an adequate measure of the beam stiffness because elementary beam theory is inadequate for dealing with the deflections of such sections where shell behavior predominates. The purpose of this investigation is to provide a correction coefficient which can be applied to the EI parameter of thin-wall truncated-cone sections and which accounts for the degeneration of stiffness from that computed by use of elementary beam theory. To achieve this specific goal, an analytical and experimental investigation of the bending characteristics of truncated conical beams subjected to end-moment loading has been made, and the results are set forth in this paper.

In reference 1 the problem of shell contribution to bending in the truncated cone has been studied, and a numerical solution for the small-deflection equations of thin conical shells under asymmetric loads has been treated.

The problem of the bending of a cantilevered thin-wall conical frustum under end moment and shear is solved in reference 2 by asymptotically integrating the equations for shell displacement. Although the analysis is exceedingly complex, results indicate that the degenerate case which reduces to the membrane theory is sufficiently accurate for many practical purposes. Consequently, membrane theory is employed in the analysis presented herein.

To verify the adequacy of the membrane theory, it was desired that corroborative experimental results be obtained from small-scale tests. To effect this testing, apparatus and range of parameter variations were held to a minimum, since the experiments were designed to investigate and verify the analytical results within engineering accuracy. In the test program, end-plane rotations of truncated cones were measured for selected values of cone angle, wall thickness, and degree of truncation.

SYMBOLS

A,B intersections of center line of test specimen and center lines of first and second magnification arms, respectively (see fig. 3)

a_c height of cone from top of truncated cone to theoretical apex, inches (centimeters)

a_t height of truncated cone, inches (centimeters)

b distance from center line of first magnification arm to base of truncated cone, inches (centimeters)

C_1,C_2,C_3,C_4 constants

D average dial-gage reading of linear deflection corresponding to relative angular deflection between ends of specimen, inches (centimeters)

d_b inside diameter at base of truncated cone, inches (centimeters)

d_e outside diameter of end of test specimen, inches (centimeters)

d_t outside diameter at top of truncated cone, inches (centimeters)

E modulus of elasticity of test specimen material, pounds/inch^2 (newtons/centimeter^2)

f	distance from center line of second magnification arm to top of truncated cone, inches (centimeters)
h	distance from center line of test specimen to center line of dial-gage arm, inches (centimeters)
I	area moment of inertia, inches^4 (centimeters^4)
k	correction coefficient to obtain effective EI on truncated conical transitions
L	length of moment arm for weights, inches (centimeters)
M	bending moment, inch-pounds (meter-newtons)
N	stress resultant, pounds/inch (newtons/centimeter)
P	load applied at end of lever arm, pounds (newtons); shear force at free end of cone
r	distance between center lines of magnification arms, inches (centimeters)
s, θ	curvilinear coordinates
t	thickness of truncated-cone wall, inches (centimeters)
u	displacement in direction of meridional coordinate s
v	displacement in direction of circumferential coordinate θ
w	displacement in direction of normal coordinate
x	coordinate, measured from theoretical apex of cone, inches (centimeters)
y	coordinate of deflection of elastic curve, inches (centimeters)
β	cone half-angle, degrees (radians)
γ	shear strain

δ overall deflection of cone

ϵ normal strain

θ relative angular rotation of specimen between end planes

μ Poisson's ratio

ξ coordinate measured from center line of first magnification arm, inches (centimeters)

ξ_1, ξ_2, ξ_3 ξ-coordinates defined in figure 3

ψ ratio of actual rotation resulting from two spans other than cone to rotation given by elementary beam theory for two spans

Subscripts:

o planar free end of analytical model

θ,s curvilinear coordinates

1 free end

2 cantilevered end of truncated cone

A tilde over a quantity denotes a separated variable.

ANALYTICAL METHOD

It has been determined that elementary beam theory becomes inadequate for determining the stiffness of truncated conical sections as the cone half-angle β increases. Employing the correction coefficient k for determining the effective stiffness parameter EI will improve calculations of flexural behavior of beams containing truncated cone spans where elementary beam theory is used. In order to compute the correction coefficient k, the results of a two-part analysis of the end-plane rotations of the truncated cone under bending loads are presented in this section. The analysis consists of (a) the membrane-theory solution and (b) the elementary-beam-theory solution. The latter

solution is the basis of comparison. The membrane-theory solution and elementary-beam-theory solution are presented in appendixes A and B, respectively, for the end-plane rotation of truncated cones. The coordinates and imposed loading used in the analytical model are shown in the descriptive sketch of the cone configuration in figure 1.

By considering only the moment contribution to the end-plane rotation in the membrane-theory solution, the stiffness constant M/θ_o can be obtained from equation (A46) as

$$\left(\frac{M}{\theta_o}\right)_{\substack{\text{membrane}\\ \text{theory}}} = \frac{\pi E t \cos^2\beta \sin^3\beta\, s_1^2}{\left(1 - \frac{s_1^2}{s_2^2}\right)\left(\frac{1}{2} + \sin^2\beta\right)} \tag{1}$$

Similarly, the moment contribution as determined by elementary beam theory can be obtained from equation (B4) as

$$\left(\frac{M}{\theta_o}\right)_{\substack{\text{beam}\\ \text{theory}}} = \frac{2\pi E t \tan\beta \sin^2\beta\, s_1^2}{\cos\beta\left(1 - \frac{s_1^2}{s_2^2}\right)} \tag{2}$$

where the membrane middle-surface coordinate is defined as

$$s = x \sec\beta \tag{3}$$

Then the correction coefficient k is defined as

$$k = \frac{\left(M/\theta_o\right)_{\substack{\text{membrane}\\ \text{theory}}}}{\left(M/\theta_o\right)_{\substack{\text{beam}\\ \text{theory}}}} = \frac{\cos^4\beta}{1 + 2\sin^2\beta} \tag{4}$$

where equation (4) is obtained by dividing equation (1) by equation (2).

APPARATUS AND TEST PROCEDURE

The small-scale test apparatus was composed of a loading stand, a test specimen, a loading device, a simple mechanism for measuring deflection, and a small shaker. The loading stand was an L-shaped angle-iron backstop which provided the foundation for the

cone specimen that had a nearly uniform bending moment applied over the test region. The specimens were maintained on a small scale to permit a full range of loading with small weights that could be easily manipulated by hand. The test specimens were truncated cones machined from 2024-T3 aluminum-alloy bar stock and had massive end sections to restrict rotations as far as possible within the boundaries of the truncated cone.

In figure 2 a photograph of the typical test apparatus and measuring device is presented. The insert in figure 2 is a photograph of the test specimen, which can also be seen mounted in the test apparatus. Details of a typical test specimen are provided in figure 3 in which the bulkiness of the overall test specimen can be compared with the cone.

The essentially uniform bending moment across the cone section was obtained by placing weights on a long lever arm as shown in figure 2. Relative angular deflections between the two ends of the specimen were measured mechanically by the use of long magnification arms attached to the heavy masses at each end of the cone. At the end of the magnification arms, the linear deflection was measured by a 0.001-inch (0.003-cm) calibrated dial gage. This measurement was converted into angular deflection by simple geometric considerations. The weight range employed in the test was 1 pound (4.448 N) to 8 pounds (35.584 N).

Due to the small deflections, the high amplifications, and the small scale of the models, considerable friction in the dial indicator was noted early in the test program. A high percentage of this friction was removed by employing a small low-frequency shaker. The shaker is indicated in figure 2. It was operated continuously during data acquisition and was effective when placed on the test bench in the vicinity of the test rig.

DISCUSSION AND PRESENTATION OF RESULTS

Figure 4 shows a typical cross section of a test specimen along with a plot of the flexibility coefficient $1/EI$ as a function of x. The $1/EI$ curves clearly show the regions that contribute significantly to the flexure. The ideal test specimen would be one that had no area under the curve except over the test span. The tests indicated that a measurable contribution to flexure also was evident in regions outside the truncated cone. This extraneous flexure, accounted for by the factor ψ was thought to result from boundary influences and ineffective material in the regions of high discontinuities near the ends of the thin-wall test sections as well as bending in the heavy foundation sections. An analytical correction process to account for these effects has been developed and is presented as appendix C.

The dimensions of each test specimen are shown in table I. The tests were made with specimens having three cone angles β, three heights a_t and distances f for each

cone angle, and three thicknesses t for each height and distance. Thus, the small-scale tests employed a total of 27 specimens.

In figure 5, plots of the averages of five sets of test data for each specimen are shown. The applied bending moment PL is plotted as a function of the angular rotation D/h. The inverse of the slopes PhL/D of the curves in figure 5 is required in the solution for k.

Equation (C8) was applied to the test curves shown in figure 5. Figure 6 shows the correction coefficient k for variations in cone half-angle β. The solid line is a plot of equation (4). It can be seen that as the cone half-angle β increases elementary beam theory becomes inadequate. The averaged results from the small-scale data for $\beta = 0^{\circ}$, 20°, and 45° as computed from equation (C8) are indicated by circles. The averaged small-scale results shown in figure 6 have no deviation for $\beta = 0^{\circ}$, whereas the dispersion for $\beta = 20^{\circ}$ and $\beta = 45^{\circ}$ is shown by the following values obtained from the tests:

$\beta = 20^{\circ}$		
a_t/d_b	t/d_b	k
0.11	0.047	0.62
.11	.033	.66
.11	.019	.68
.23	.047	.70
.23	.033	.69
.23	.019	.71
.32	.047	.64
.32	.033	.64
.32	.019	.63
Average		0.663

$\beta = 45^{\circ}$		
a_t/d_b	t/d_b	k
0.11	0.047	0.13
.11	.033	.15
.11	.019	.12
.23	.047	.16
.23	.033	.15
.23	.019	.14
.32	.047	.13
.32	.033	.13
.32	.019	.13
Average		0.138

An analytically computed value for k has been determined from a numerical example available in reference 1 and is shown by the square in figure 6.

CONCLUDING REMARKS

An analytical and experimental investigation of the bending characteristics of truncated conical beams subjected to constant moment loading has been made. It has been determined that elementary beam theory becomes inadequate for determining the stiffness of truncated conical sections as the cone half-angle increases. Employing the correction coefficient for determining the effective stiffness parameter EI will improve calculations of flexural behavior of beams containing truncated cone spans where elementary

beam theory is used. The experimentally determined values of the correction coefficient show reasonably good agreement with the analytically determined values.

Langley Research Center,
National Aeronautics and Space Administration,
Langley Station, Hampton, Va., August 6, 1969.

APPENDIX A

MEMBRANE-THEORY SOLUTION FOR A TRUNCATED CONE SUBJECTED TO END-PLANE ROTATIONS

The membrane-theory solution for a truncated cone subjected to end-plane rotations is derived in this appendix. The coordinate system and the loading conditions for the analytical model are as shown in figure 1. The equations of equilibrium obtained from reference 2 are

$$\frac{\partial}{\partial s}\left(sN_s \sin \beta\right) + \frac{\partial}{\partial \theta} N_{\theta s} = 0 \tag{A1}$$

$$\frac{\partial}{\partial s}\left(sN_{s\theta} \sin \beta\right) + N_{\theta s} \sin \beta = 0 \tag{A2}$$

$$N_\theta = 0 \tag{A3}$$

The stress-strain relations are

$$N_s = \frac{Et}{1 - \mu^2}\left(\epsilon_s + \mu\epsilon_\theta\right) \tag{A4}$$

$$N_\theta = \frac{Et}{1 - \mu^2}\left(\epsilon_\theta + \mu\epsilon_s\right) \tag{A5}$$

$$N_{s\theta} = \frac{1 - \mu}{2} \frac{Et}{1 - \mu^2} \gamma_{s\theta} \tag{A6}$$

The strain-displacement relations are

$$\epsilon_s = \frac{\partial u}{\partial s} \tag{A7}$$

$$\epsilon_\theta = \frac{1}{s \sin \beta} \frac{\partial v}{\partial \theta} + \frac{u - w \cot \beta}{s} \tag{A8}$$

$$\gamma_{s\theta} = \frac{\partial v}{\partial s} - \frac{v}{s} + \frac{1}{s \sin \beta} \frac{\partial u}{\partial \theta} \tag{A9}$$

Equating equations (A3) and (A5) yields

$$\epsilon_\theta = -\mu\epsilon_s \tag{A10}$$

Utilizing equations (A10) and (A7) in equation (A4) yields

$$N_s = \frac{Et}{1 - \mu^2}\left(1 - \mu^2\right)\frac{\partial u}{\partial s} \tag{A11}$$

Substitution of equation (A9) into equation (A6) yields

$$N_{s\theta} = \frac{1 - \mu}{2}\frac{Et}{1 - \mu^2}\left(\frac{\partial v}{\partial s} - \frac{v}{s} + \frac{1}{s \sin \beta}\frac{\partial u}{\partial \theta}\right) \tag{A12}$$

Also, after substitution of equations (A7) and (A8), equation (A10) becomes

$$\frac{1}{s \sin \beta}\frac{\partial v}{\partial \theta} + \frac{u - w \cot \beta}{s} + \mu \frac{\partial u}{\partial s} = 0 \tag{A13}$$

Now, by assuming displacements of the form

$$u(s, \theta) = \tilde{u}(s)\cos \theta \tag{A14a}$$

$$v(s, \theta) = \tilde{v}(s)\sin \theta \tag{A14b}$$

$$w(s, \theta) = \tilde{w}(s)\cos \theta \tag{A14c}$$

and by making use of equations (A11) to (A13), equations (A4) to (A6) become

$$N_s(s, \theta) = \tilde{N}_s(s)\cos \theta \tag{A15a}$$

$$N_{s\theta}(s, \theta) = \tilde{N}_{s\theta}(s)\sin \theta \tag{A15b}$$

$$N_\theta(s, \theta) = \tilde{N}_\theta(s)\cos \theta \tag{A15c}$$

Thus, the equilibrium equations (A1) and (A2), after substitution of equations (A15a), (A15b), and (A15c) become

$$\frac{d}{ds}\left(s\tilde{N}_s \sin \beta\right) + \tilde{N}_{s\theta} = 0 \tag{A16}$$

and

$$\frac{d}{ds}\left(s\tilde{N}_{s\theta} \sin \beta\right) + \tilde{N}_{s\theta} \sin \beta = 0 \tag{A17}$$

Equation (A17) can be written as

$$\frac{d}{ds}\left(s^2\tilde{N}_{s\theta}\right) = 0 \tag{A18}$$

or upon integrating

$$\tilde{N}_{s\theta}(s) = \frac{C_1}{s^2} \tag{A19}$$

Also, substituting equation (A19) into equation (A16) yields

$$\frac{d}{ds}\left(s\tilde{N}_s \sin\beta\right) + \frac{C_1}{s^2} = 0 \tag{A20}$$

or upon integrating

$$\tilde{N}_s(s) = \frac{C_1}{s^2 \sin\beta} + \frac{C_2}{s \sin\beta} \tag{A21}$$

Equating equation (A21) to equation (A11) yields

$$\frac{d\tilde{u}}{ds} = \frac{1}{Et}\left(\frac{C_1}{s^2 \sin\beta} + \frac{C_2}{s \sin\beta}\right) \tag{A22}$$

or

$$\tilde{u}(s) = \frac{1}{Et}\left(-\frac{C_1}{s \sin\beta} + \frac{C_2}{\sin\beta} \ln s + C_3\right) \tag{A23}$$

The boundary conditions for a truncated cone subjected to end-plane rotations are (fig. 1)

$$u(s_1) = -\left(\theta_o s_1 \cos\beta + \delta_o\right)\sin\beta \cos\theta \tag{A24a}$$

$$v(s_1) = \delta_o \sin\theta \tag{A24b}$$

$$w(s_1) = \left(\delta_o \cos\beta - \theta_o s_1 \sin^2\beta\right)\cos\theta \tag{A24c}$$

at $s = s_1$ and

$$u(s_2) = v(s_2) = w(s_2) = 0 \tag{A25}$$

at $s = s_2$.

By utilizing equations (A14a), (A14b), and (A14c), equations (A24a), (A24b), and (A24c) can be written in matrix form and inverted to obtain

$$\begin{Bmatrix} \theta_o \\ \delta_o \end{Bmatrix} = \begin{bmatrix} -\frac{\cos\beta}{s_1} & -\frac{1}{s_1} \\ -\sin^2\beta & \cos\beta \end{bmatrix} \begin{Bmatrix} \frac{\tilde{u}(s_1)}{\sin\beta} \\ \tilde{w}(s_1) \end{Bmatrix} \tag{A26}$$

Evaluating equation (A23) at $s = s_2$ and using equation (A25) yield

$$C_3 = \frac{C_1}{s_2 \sin\beta} - \frac{C_2 \ln s_2}{\sin\beta} \tag{A27}$$

Substituting equation (A27) into equation (A23) yields

$$\tilde{u}(s) = \frac{1}{Et \sin\beta}\left[C_1\left(\frac{1}{s_2} - \frac{1}{s}\right) - C_2 \ln\frac{s_2}{s_1}\right] \tag{A28}$$

Substituting equation (A19) into equation (A12) yields

$$\frac{d\tilde{v}}{ds} - \frac{\tilde{v}}{s} = \frac{2(1+\mu)C_1}{Ets^2} + \frac{\tilde{u}}{s \sin\beta} \tag{A29}$$

and using equation (A28) yields

$$\frac{\tilde{v}}{s} = \frac{1}{Et \sin^2\beta}\left\{\frac{C_1}{s^2}\left[\frac{1}{2} - \sin^2\beta(1+\mu)\right] - \frac{C_1}{ss_2} + \frac{C_2}{s}\left(\ln\frac{s_2}{s} - 1\right)\right\} + C_4 \tag{A30}$$

Of the three conditions given in equation (A25), only two can be satisfied simultaneously. The two conditions to be satisfied are

$$\left.\begin{aligned} \tilde{u}(s_2) = \tilde{w}(s_2) = 0 \\ \tilde{v}(s_2) \approx 0 \end{aligned}\right\} \tag{A31}$$

Equation (A13) can be written

$$\tilde{w}(s) = \frac{s}{\cot\beta}\left(\frac{\tilde{v}}{s \sin\beta} + \frac{\tilde{u}}{s} + \mu\frac{d\tilde{u}}{ds}\right) \tag{A32}$$

Substituting equations (A22), (A28), and (A30) into equation (A32) yields

$$\tilde{w}(s) = \frac{1}{Et \cos \beta}\left\{C_1\left[\frac{1}{s}\left(\frac{1}{2 \sin^2\beta} - 2\right) + \frac{1}{s_2}\left(1 - \frac{1}{\sin^2\beta}\right)\right]\right.$$

$$\left. + C_2\left[\left(\frac{1}{\sin^2\beta} - 1\right)\ln\frac{s_2}{s} + \mu - \frac{1}{\sin^2\beta}\right] + C_4 sEt\right\} \tag{A33}$$

Evaluating equation (A33) at $s = s_2$ and using equation (A31) yield

$$C_4 = \frac{1}{Et \sin^2\beta}\left[\frac{C_1}{{s_2}^2}\left(\frac{1}{2} + \sin^2\beta\right) + \frac{C_2}{s_2}\left(1 - \mu \sin^2\beta\right)\right] \tag{A34}$$

Substituting equation (A34) into equation (A33) yields

$$\tilde{w}(s) = \frac{1}{Et \cos \beta \sin^2\beta}\left\{C_1\left[\frac{s}{{s_2}^2}\left(\frac{1}{2} + \sin^2\beta\right) + \frac{1}{s}\left(\frac{1}{2} - 2 \sin^2\beta\right) - \frac{\cos^2\beta}{s_2}\right]\right.$$

$$\left. + C_2\left[\cos^2\beta \ln\frac{s_2}{s_1} + \left(1 - \frac{s}{s_2}\right)\left(\mu \sin^2\beta - 1\right)\right]\right\} \tag{A35}$$

For overall equilibrium of the truncated cone

$$\int_0^{2\pi} \left(N_s \cos \theta \sin \beta - N_{s\theta} \sin \theta\right) s \sin \beta \, d\theta = P \tag{A36}$$

and

$$\int_0^{2\pi} N_s \cos \theta s^2 \sin^2\beta \cos \beta \, d\theta = M + P\left(s - s_1\right)\cos \beta \tag{A37}$$

Integrating equations (A36) and (A37) at $s = s_1$ yields

$$P = \pi s_1 \sin^2\beta \, \tilde{N}_s\left(s_1\right) - \pi s_1 \sin \beta \, \tilde{N}_{s\theta}\left(s_1\right) \tag{A38}$$

and

$$M = N_s\left(s_1\right)\pi {s_1}^2 \sin^2\beta \cos \beta \tag{A39}$$

Evaluating equations (A19) and (A21) at $s = s_1$ yields

$$\tilde{N}_{s\theta}(s_1) = \frac{C_1}{s_1^2} \tag{A40}$$

and

$$\tilde{N}_s(s_1) = \frac{C_1}{s_1^2 \sin\beta} + \frac{C_2}{s_1 \sin\beta} \tag{A41}$$

and substituting equations (A40) and (A41) into equations (A38) and (A39) yields

$$C_1 = \frac{M}{\pi \sin\beta \cos\beta} - \frac{Ps_1}{\pi \sin\beta} \tag{A42}$$

and

$$C_2 = \frac{P}{\pi \sin\beta} \tag{A43}$$

Substituting equations (A41) and (A42) into equations (A28) and (A35) and evaluating at $s = s_1$ yield

$$\frac{\tilde{u}(s_1)}{\sin\beta} = \frac{1}{\pi Et \cos\beta \sin^3\beta}\left\{M\left(\frac{1}{s_2} - \frac{1}{s_1}\right) - Ps_1 \cos\beta\left[\left(\frac{1}{s_2} - \frac{1}{s_1}\right) + \frac{1}{s_1}\ln\frac{s_2}{s_1}\right]\right\} \tag{A44}$$

and

$$\tilde{w}(s_1) = \frac{1}{\pi Et \cos\beta \sin^3\beta}\left\{\frac{M}{\cos\beta}\left[\frac{s_1}{s_2^2}\left(\frac{1}{2} + \sin^2\beta\right) + \frac{1}{s_1}\left(\frac{1}{2} - 2\sin^2\beta\right) - \frac{\cos^2\beta}{s_2}\right] + P\left[\cos^2\beta \ln\frac{s_2}{s_1}\right.\right.$$

$$\left.\left. + \left(1 - \frac{s_1}{s_2}\right)\left(\mu \sin^2\beta - 1\right) - \frac{s_1^2}{s_2^2}\left(\frac{1}{2} + \sin^2\beta\right) - \left(\frac{1}{2} - 2\sin^2\beta\right) + \frac{s_1}{s_2}\cos^2\beta\right]\right\} \tag{A45}$$

By substituting equations (A44) and (A45) into equation (A26) and solving for the planar rotation, θ_o can be written

$$\theta_O = \frac{\left(1 - \frac{s_1^2}{s_2^2}\right)\left(\frac{1}{2} + \sin^2\beta\right)M}{\pi Et \cos^2\beta \sin^3\beta\, s_1^2} + \frac{s_1 \cos\beta P}{\pi Et \cos^2\beta \sin^3\beta\, s_1^2}\left[\left(1 - \frac{s_1}{s_2}\right)\left(1 - \mu \sin^2\beta\right)\right.$$

$$\left. - \left(1 - \frac{s_1^2}{s_2^2}\right)\left(\frac{1}{2} + \sin^2\beta\right)\right] \qquad \text{(A46)}$$

APPENDIX B

ELEMENTARY-BEAM-THEORY SOLUTION FOR TRUNCATED CONE SUBJECTED TO END-PLANE ROTATIONS

In this appendix elementary beam theory is used to describe cone rotations. The solution for the cone section (fig. 1) is obtained from the equation

$$EI \frac{d}{dx}\left(\frac{d\delta}{dx}\right) = M + P(x - x_1) \tag{B1}$$

For thin-shell sections the moment of inertia of the cone cross section can be approximated by

$$I \approx \pi \frac{t}{\cos \beta}(x \tan \beta)^3 \tag{B2}$$

Substituting equation (B2) into equation (B1) yields

$$\frac{d}{dx}\left(\frac{d\delta}{dx}\right) = \frac{M + P(x - x_1)}{E\pi t x^3 \frac{\tan^3 \beta}{\cos \beta}} \tag{B3}$$

Integrating equation (B3) between the limits of $x = x_1$ and $x = x_2$ results in

$$\theta_O = \frac{d\delta}{dx} = \frac{\cos \beta}{2\pi E t \tan \beta \, (x \tan \beta)^2}\left[M\left(1 - \frac{x_1^2}{x_2^2}\right) + P x_1\left(1 - \frac{x_1}{x_2}\right)^2\right] \tag{B4}$$

APPENDIX C

ANALYSIS PERTINENT TO BOUNDARY INFLUENCES ON EXPERIMENTAL RESULTS

The expressions which were used for reducing experimental data are presented in this appendix. For the small-scale models an attempt was made to eliminate the boundary influences in order to determine the reduction in EI for the conical section only.

The stiffness deviation of the cone section from that computed by use of elementary beam theory is represented by the factor $1/k$, and the influences of the boundaries are accounted for by the factor ψ which also includes the influences of ineffective material in the regions of high discontinuities near the ends of the thin-wall test sections as well as bending in the heavy foundation sections. From the experimental flexural-load curves and from the flexural-load data for the cylindrical case, the $1/k$ and ψ values were calculated. The ψ values were assumed to remain constant for variations in cone angle.

The equations used for eliminating the boundary flexure contributions and the expression for the cone stiffness factor are developed in the following paragraphs. The basic geometry and the coordinate system are shown in figure 3.

The moment at position ξ due to a concentrated load at L is

$$M = P(L - \xi) \tag{C1}$$

From elementary beam theory

$$EI \frac{d^2y}{d\xi^2} = P(L - \xi) \tag{C2}$$

By dividing the span into three spans of interest (i.e., $0 \leqq \xi \leqq \xi_1$, $\xi_1 \leqq \xi \leqq \xi_2$, $\xi_2 \leqq \xi \leqq \xi_3$), the relative rotation between A and B can be expressed as

$$(\theta)_{\substack{\text{ideal} \\ \text{beam} \\ \text{rotation}}} = P\left(\int_0^{\xi_1} \frac{L - \xi}{EI} d\xi + \int_{\xi_1}^{\xi_2} \frac{L - \xi}{EI} d\xi + \int_{\xi_2}^{\xi_3} \frac{L - \xi}{EI} d\xi\right) \tag{C3}$$

Now, consider that the rotation contribution in the middle span is altered by virtue of combined elementary bending and shell flexure. Let the constant $1/k$ represent the ratio of the actual rotation contribution of the central span to the elementary beam

rotation given by the second integral in equation (C3). Also, all deviations from simple beam theory in the boundary sections $0 \leqq \xi \leqq \xi_1$ and $\xi_2 \leqq \xi \leqq \xi_3$ are accounted for by the modifying factor ψ.

Equation (C3) can now be modified to read

$$\theta = P\left(\psi \int_0^{\xi_1} \frac{L - \xi}{EI}\, d\xi + \frac{1}{k}\int_{\xi_1}^{\xi_2} \frac{L - \xi}{EI}\, d\xi + \psi \int_{\xi_2}^{\xi_3} \frac{L - \xi}{EI}\, d\xi\right) \tag{C4}$$

From the test data, θ can be expressed in terms of observed results as

$$\theta = \frac{D}{h} \tag{C5}$$

Substitution of equation (C5) into equation (C4) gives

$$\frac{D}{PhL} = \psi\left(\int_0^{\xi_1} \frac{1 - \frac{\xi}{L}}{EI}\, d\xi + \int_{\xi_2}^{\xi_3} \frac{1 - \frac{\xi}{L}}{EI}\, d\xi\right) + \frac{1}{k}\int_{\xi_1}^{\xi_2} \frac{1 - \frac{\xi}{L}}{EI}\, d\xi \tag{C6}$$

In order to establish ψ, consideration is given to the limiting cone case (i.e., the cylinder ($\beta = 0^o$)). For the cylindrical shell, the flexural characteristics over the span ξ_1 to ξ_2 are considered reasonably well approximated by elementary beam theory. Hence, for the cylindrical case only ($\beta = 0^o$), $1/k$ is assumed to be equal to unity, and this assumption permits a solution for ψ, that is,

$$\psi = \frac{\frac{D_{\beta=0}}{PhL} - \int_{\xi_1}^{\xi_2} \frac{1 - \frac{\xi}{L}}{EI}\, d\xi}{\int_0^{\xi_1} \frac{1 - \frac{\xi}{L}}{EI}\, d\xi + \int_{\xi_2}^{\xi_3} \frac{1 - \frac{\xi}{L}}{EI}\, d\xi} \tag{C7}$$

After ψ is obtained, the value for k can be obtained for any desired cone from equation (C6) by means of the equation

$$k = \frac{\int_{\xi_1}^{\xi_2} \frac{1 - \frac{\xi}{L}}{EI}\, d\xi}{\frac{D}{PhL} - \psi\left(\int_0^{\xi_1} \frac{1 - \frac{\xi}{L}}{EI}\, d\xi + \int_{\xi_2}^{\xi_3} \frac{1 - \frac{\xi}{L}}{EI}\, d\xi\right)} \tag{C8}$$

Equations (C7) and (C8) provide relationships for obtaining approximate modifying factors that can be applied to the EI values.

REFERENCES

1. Thurston, Gaylen A.: A Numerical Solution for Thin Conical Shells Under Asymmetrical Loads. 4th Midwestern Conference on Solid Mechanics, Univ. of Texas, 1959, pp. 171-194.

2. Seide, Paul: On the Bending of Cantilevered Thin-Walled Conical Frustrums by End Loads. GM-TR-284, The Ramo-Wooldridge Corp., Dec. 15, 1957.

TABLE I.- DIMENSIONS OF TEST SPECIMENS

(a) U.S. Customary Units

[b = 0.850 in.; d_e = 3.0 in.; r = 3.525 in.]

Specimen	Dimension								
	a_t, in.	β, deg	a_c, in.	d_t, in.	f, in.	h, in.	d_b, in.	L, in.	t, in.
1	0.175	45	0.883	1.500	2.500	32.50	1.765	24.47	0.030
2	.350	45	.884	1.150	2.325	32.50	1.767	24.69	.029
3	.500	45	.883	.850	2.175	32.50	1.765	24.69	.030
4	.175	45	.855	1.500	2.500	32.50	1.709	24.81	.050
5	.350	45	.856	1.150	2.325	32.53	1.711	24.97	.049
6	.500	45	.852	.850	2.175	32.50	1.704	24.75	.052
7	.175	45	.824	1.525	2.500	32.50	1.673	24.56	.072
8	.350	45	.820	1.150	2.325	32.53	1.639	24.91	.075
9	.500	45	.821	.850	2.175	32.50	1.641	24.84	.074
10	.175	20	2.148	1.500	2.500	32.50	1.564	24.75	.030
11	.350	20	2.146	1.372	2.325	32.53	1.562	24.97	.030
12	.500	20	2.146	1.263	2.175	32.50	1.562	24.69	.030
13	.175	20	2.088	1.500	2.500	32.50	1.520	24.69	.050
14	.350	20	2.092	1.372	2.325	32.53	1.523	25.00	.049
15	.500	20	2.083	1.263	2.175	32.47	1.517	24.66	.052
16	.175	20	2.025	1.500	2.500	32.50	1.474	24.63	.072
17	.350	20	2.037	1.372	2.325	32.56	1.483	24.84	.068
18	.500	20	2.032	1.263	2.175	32.50	1.479	24.66	.069
19	.175	0	∞	1.501	2.500	32.50	1.441	24.69	.030
20	.350	0	∞	1.500	2.325	32.56	1.446	24.91	.027
21	.500	0	∞	1.500	2.175	32.50	1.446	24.72	.027
22	.175	0	∞	1.501	2.500	32.50	1.401	24.75	.050
23	.350	0	∞	1.501	2.325	32.53	1.400	24.84	.051
24	.500	0	∞	1.501	2.175	32.50	1.400	24.63	.050
25	.175	0	∞	1.499	2.500	32.50	1.363	24.69	.068
26	.350	0	∞	1.495	2.325	32.53	1.355	24.91	.070
27	.500	0	∞	1.495	2.175	32.50	1.357	24.75	.069

TABLE I.- DIMENSIONS OF TEST SPECIMENS – Concluded

(b) SI Units

[b = 2.159 cm; d_e = 7.620 cm; r = 8.954 cm]

Specimen	Dimension								
	a_t, cm	β, rad	a_c, cm	d_t, cm	f, cm	h, cm	d_b, cm	L, cm	t, cm
1	0.445	0.785	2.243	3.810	6.350	82.55	4.483	62.15	0.076
2	.889	.785	2.245	2.921	5.906	82.55	4.488	62.71	.074
3	1.270	.785	2.243	2.159	5.525	82.55	4.483	62.71	.076
4	.445	.785	2.172	3.810	6.350	82.55	4.341	63.02	.127
5	.889	.785	2.174	2.921	5.906	82.63	4.346	63.42	.124
6	1.270	.785	2.164	2.159	5.525	82.55	4.328	62.87	.132
7	.445	.785	2.093	3.874	6.350	82.55	4.249	62.38	.183
8	.889	.785	2.083	2.921	5.906	82.63	4.163	63.27	.191
9	1.270	.785	2.085	2.159	5.525	82.55	4.168	63.09	.188
10	.445	.349	5.456	3.810	6.350	82.55	3.973	62.87	.076
11	.889	.349	5.451	3.485	5.906	82.63	3.967	63.42	.076
12	1.270	.349	5.451	3.208	5.525	82.55	3.967	62.71	.076
13	.445	.349	5.304	3.810	6.350	82.55	3.861	62.71	.127
14	.889	.349	5.314	3.485	5.906	82.63	3.868	63.50	.124
15	1.270	.349	5.291	3.208	5.525	82.47	3.853	62.64	.132
16	.445	.349	5.144	3.810	6.350	82.55	3.744	62.56	.183
17	.889	.349	5.174	3.485	5.906	82.70	3.767	63.09	.173
18	1.270	.349	5.161	3.208	5.525	82.55	3.757	62.64	.175
19	.445	0	∞	3.813	6.350	82.55	3.660	62.71	.076
20	.889	0	∞	3.810	5.906	82.70	3.673	63.27	.069
21	1.270	0	∞	3.810	5.525	82.55	3.673	62.79	.069
22	.445	0	∞	3.813	6.350	82.55	3.559	62.87	.127
23	.889	0	∞	3.813	5.906	82.63	3.556	63.09	.130
24	1.270	0	∞	3.813	5.525	82.55	3.556	62.56	.127
25	.445	0	∞	3.807	6.350	82.55	3.462	62.71	.173
26	.889	0	∞	3.797	5.906	82.63	3.442	63.27	.178
27	1.270	0	∞	3.797	5.525	82.55	3.447	62.87	.175

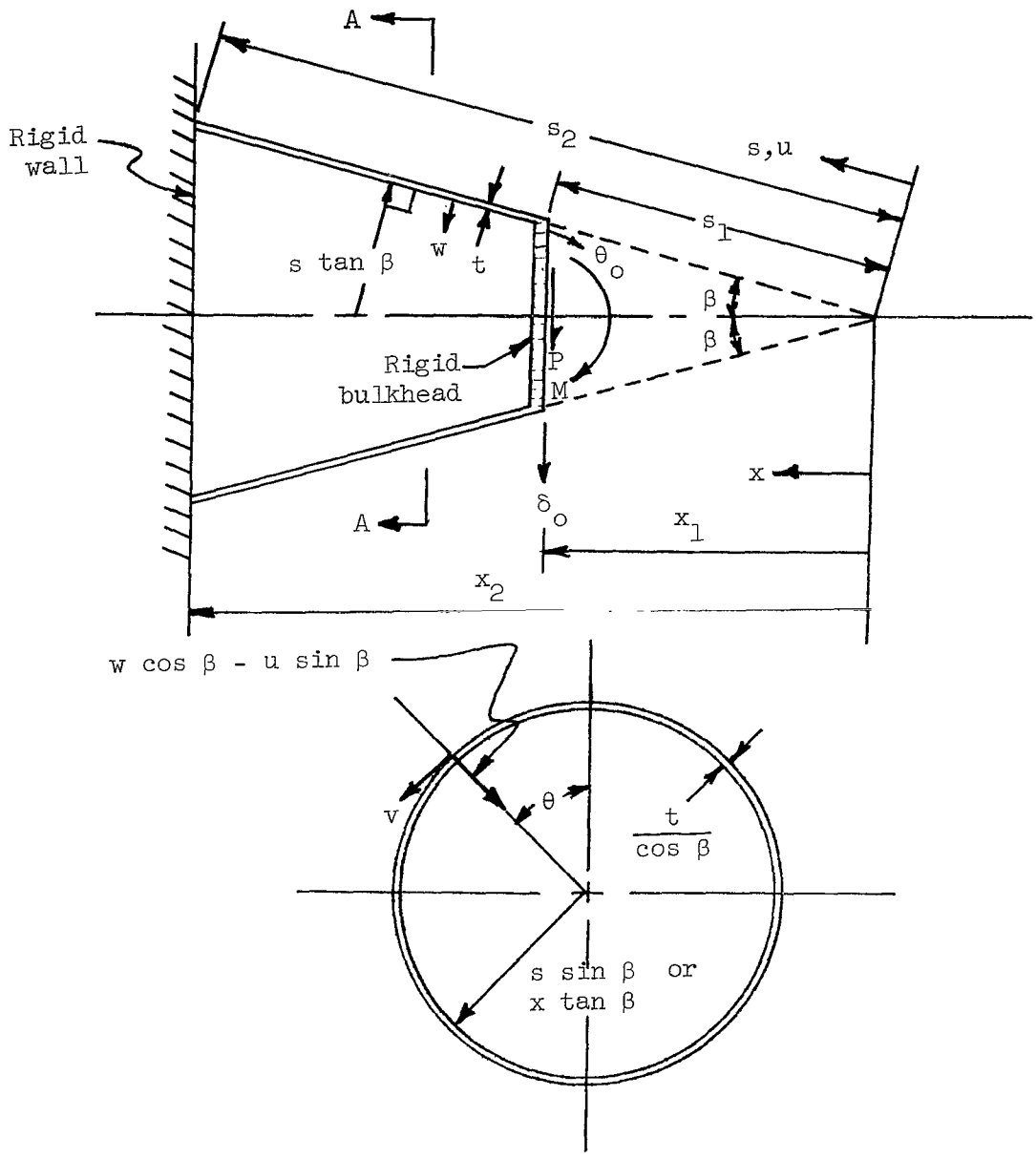

Figure 1.- Analytical model.

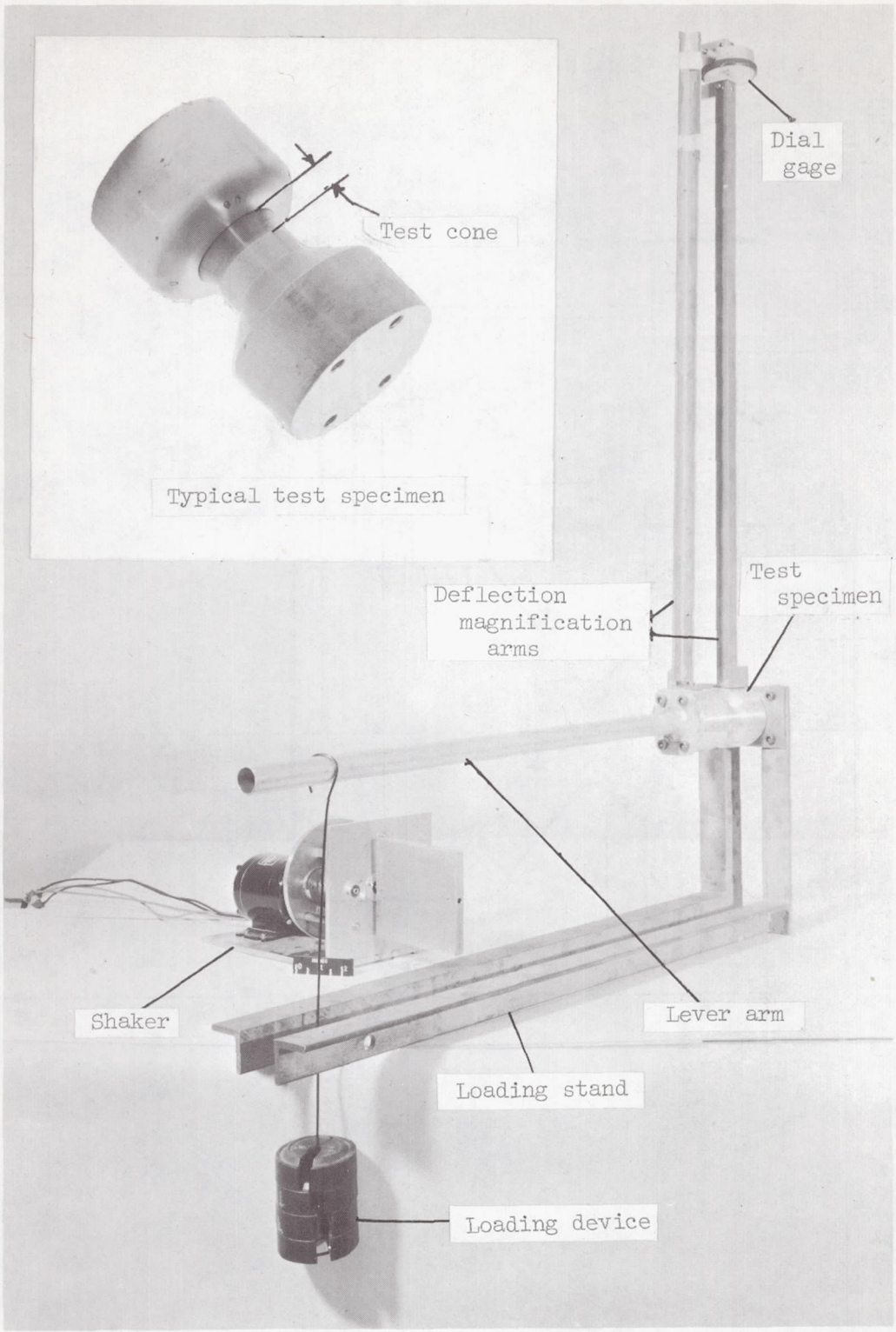

Figure 2.- Apparatus for loading and measuring conical beam specimens. L-69-5075

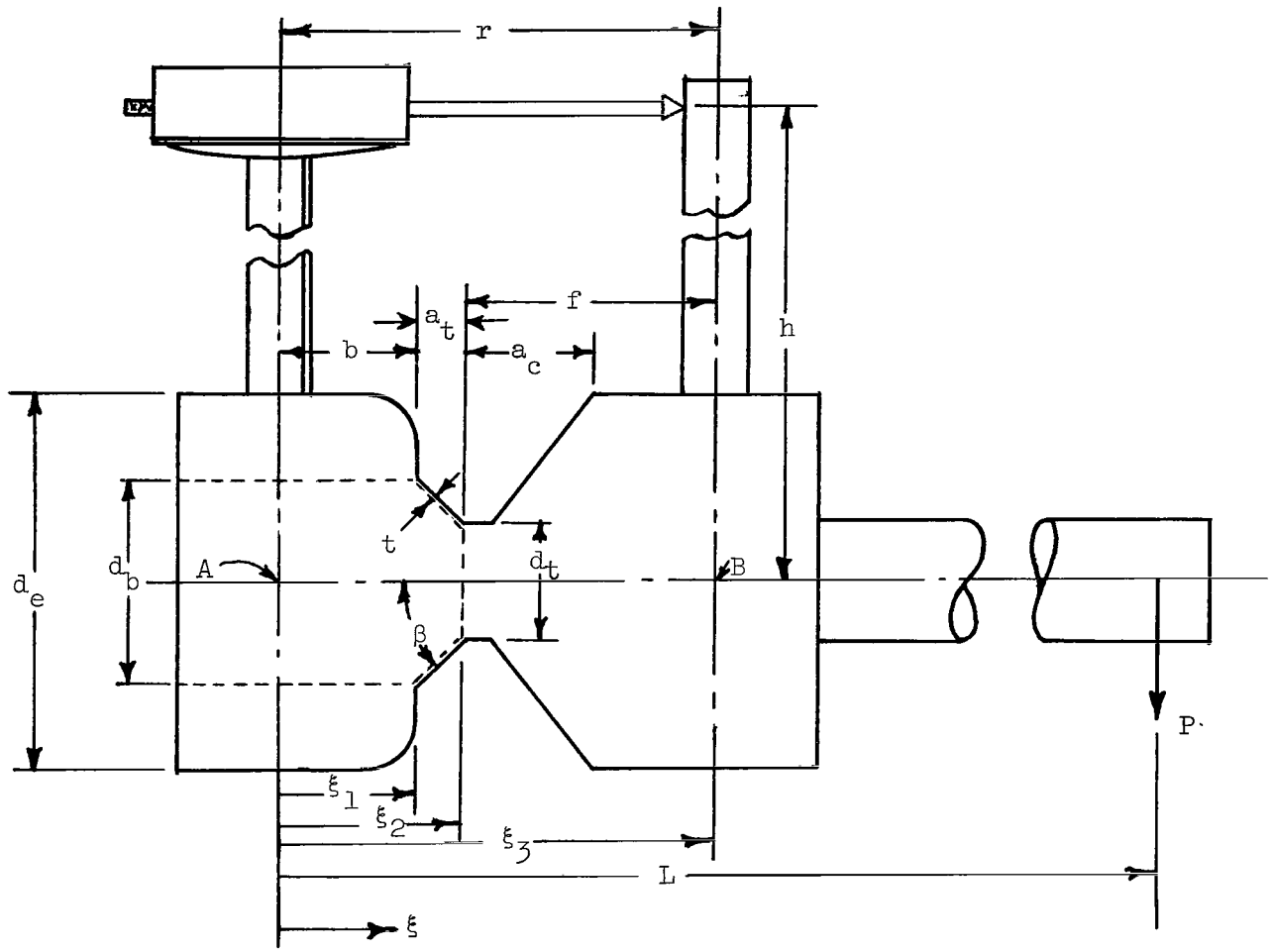

Figure 3.- Detail of a typical test specimen.

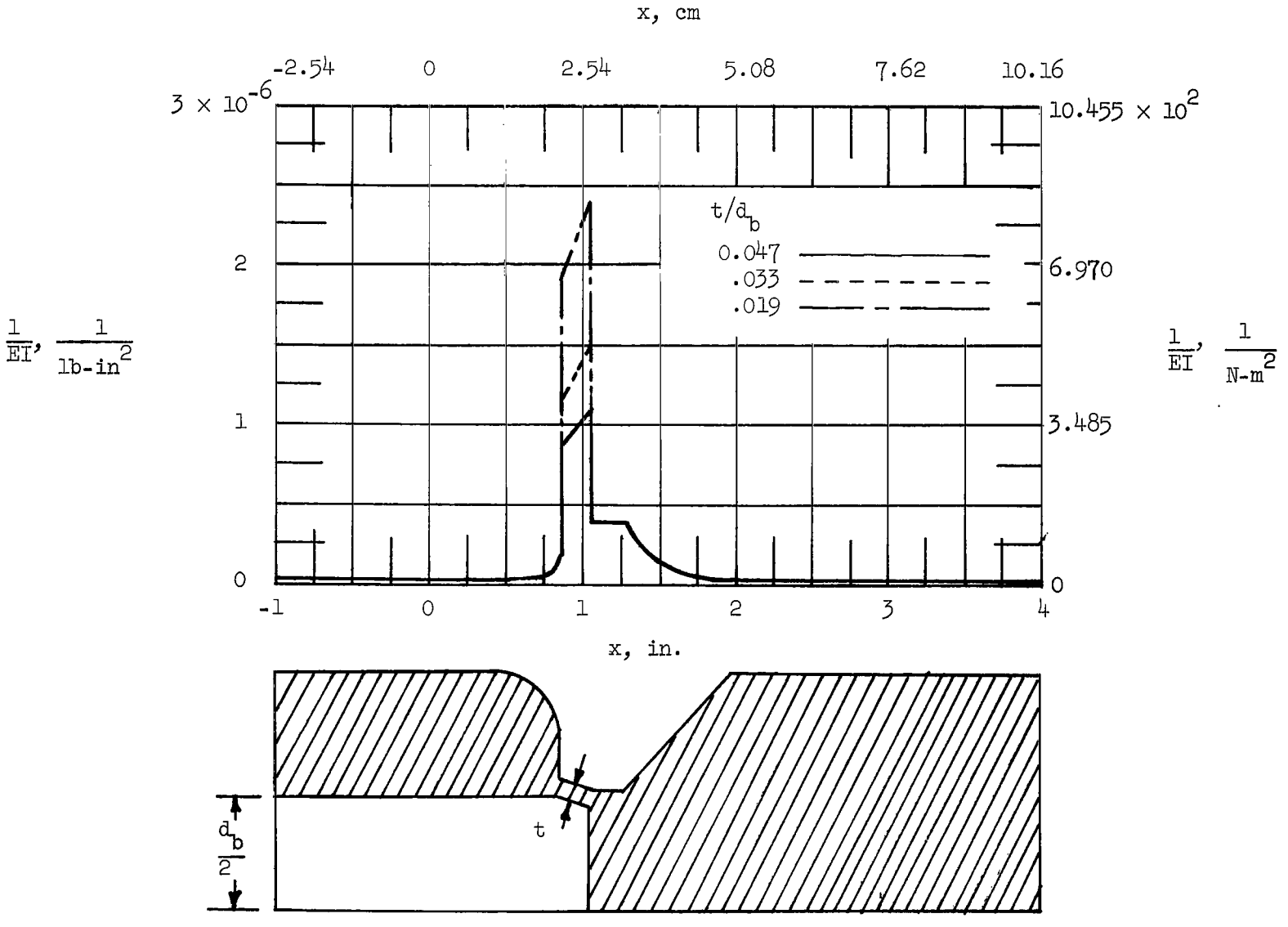

Figure 4.- Typical test-specimen flexibility coefficients $1/EI$. $a_t/d_b = 0.11$; $\beta = 20^0$.

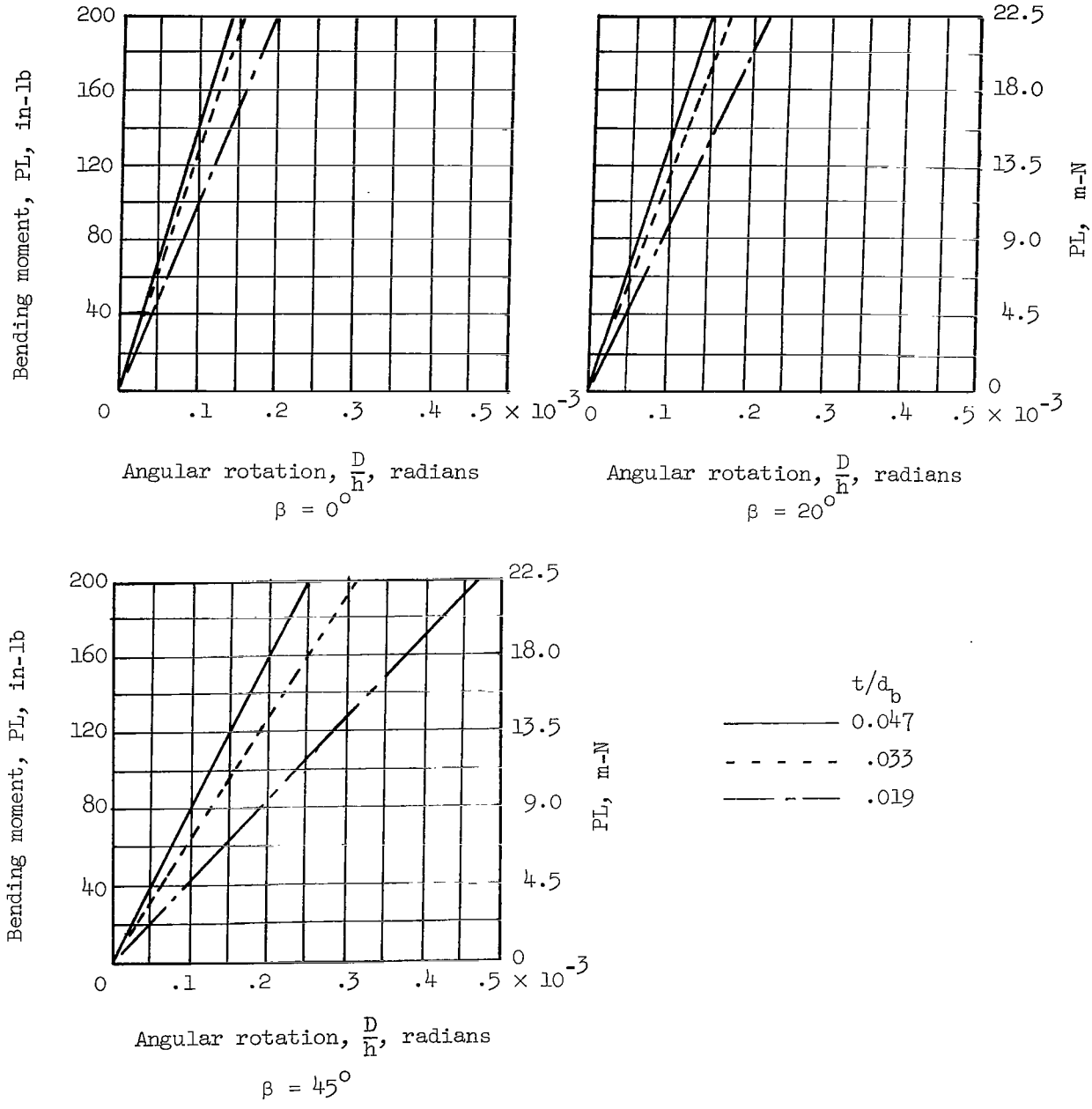

(a) $a_t/d_b = 0.11$.

Figure 5.- Plots of averages of test data.

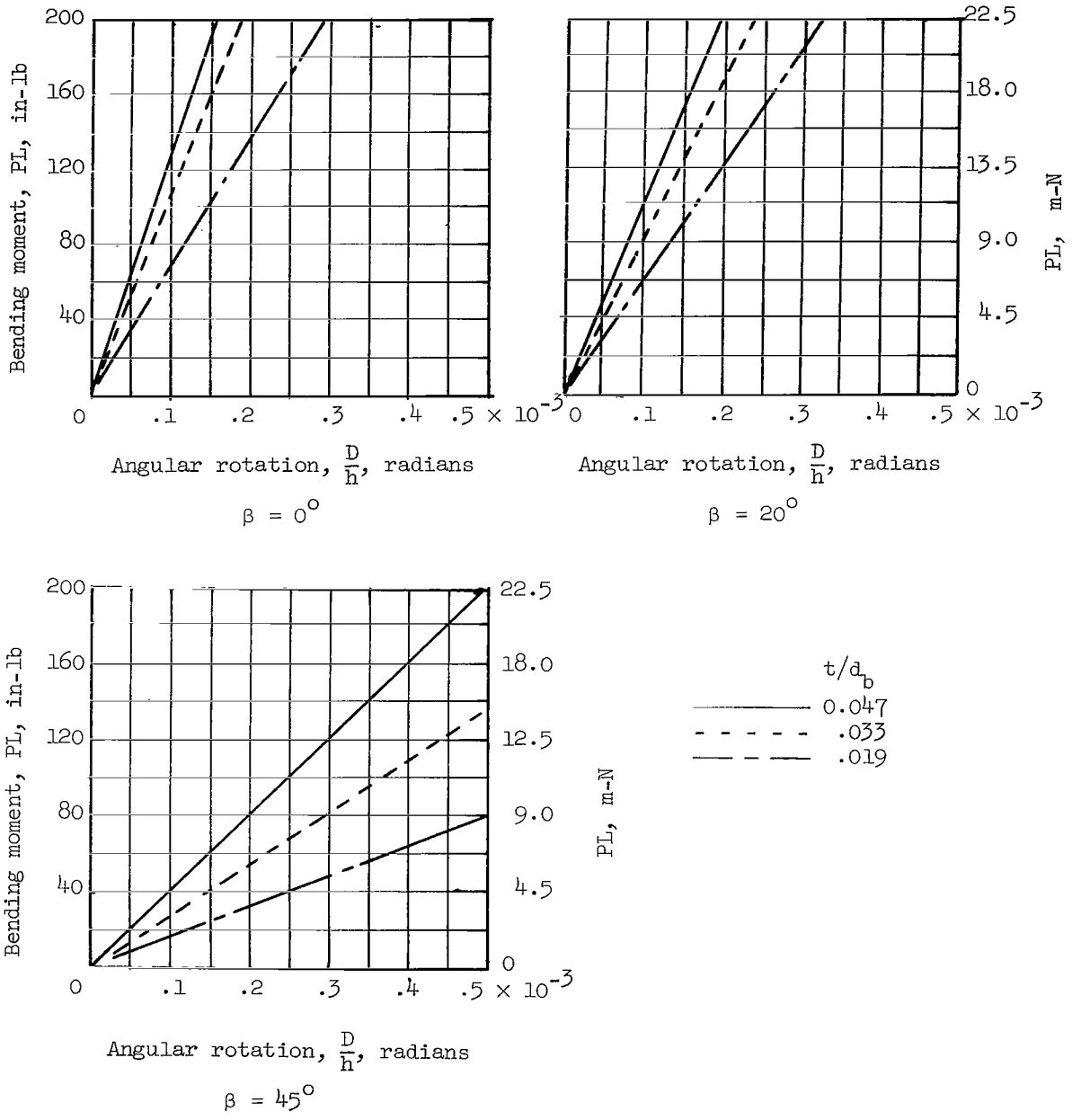

(b) $a_t/d_b = 0.23$.

Figure 5.- Continued.

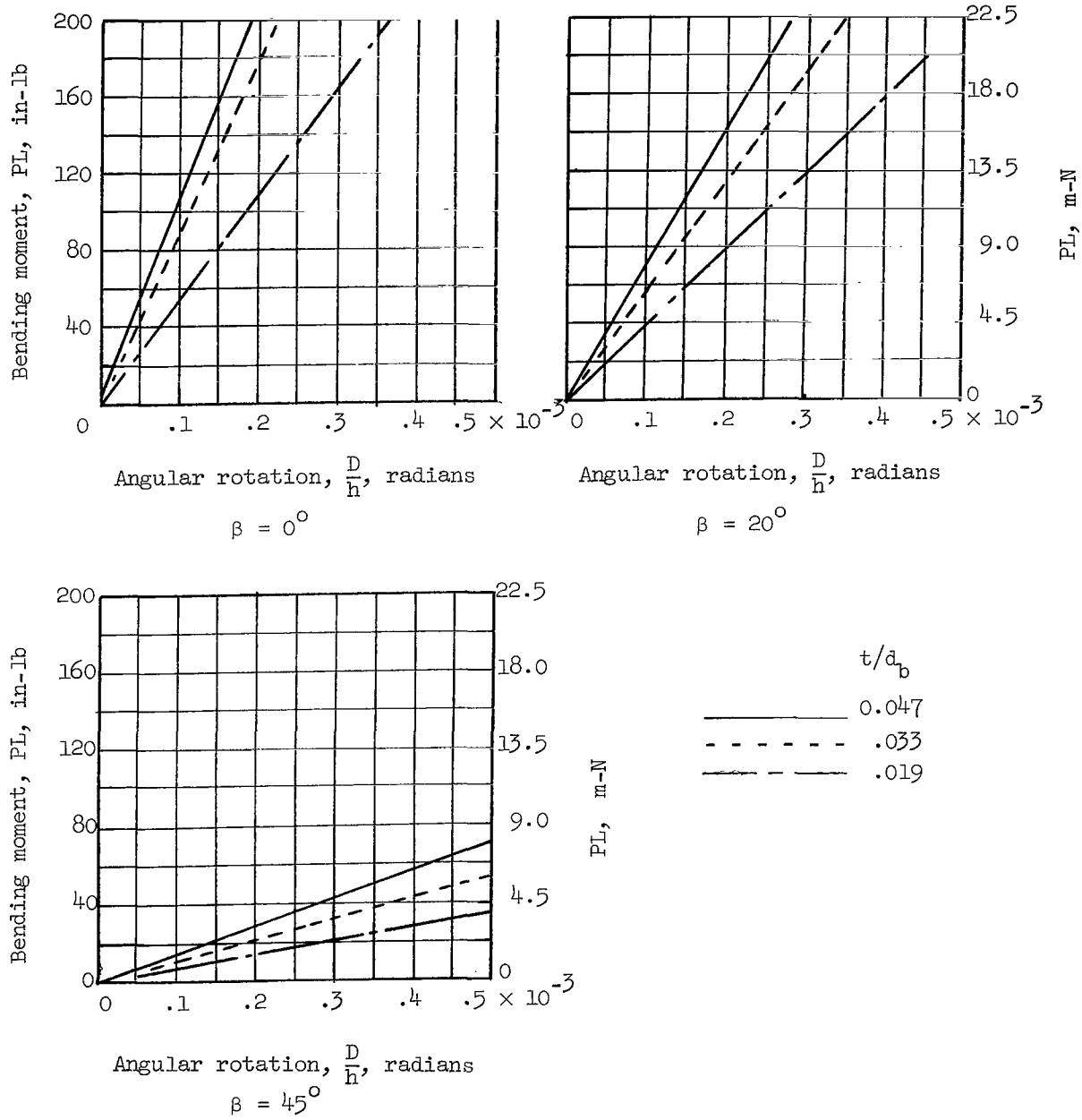

(c) $a_t/d_b = 0.32$.

Figure 5.- Concluded.

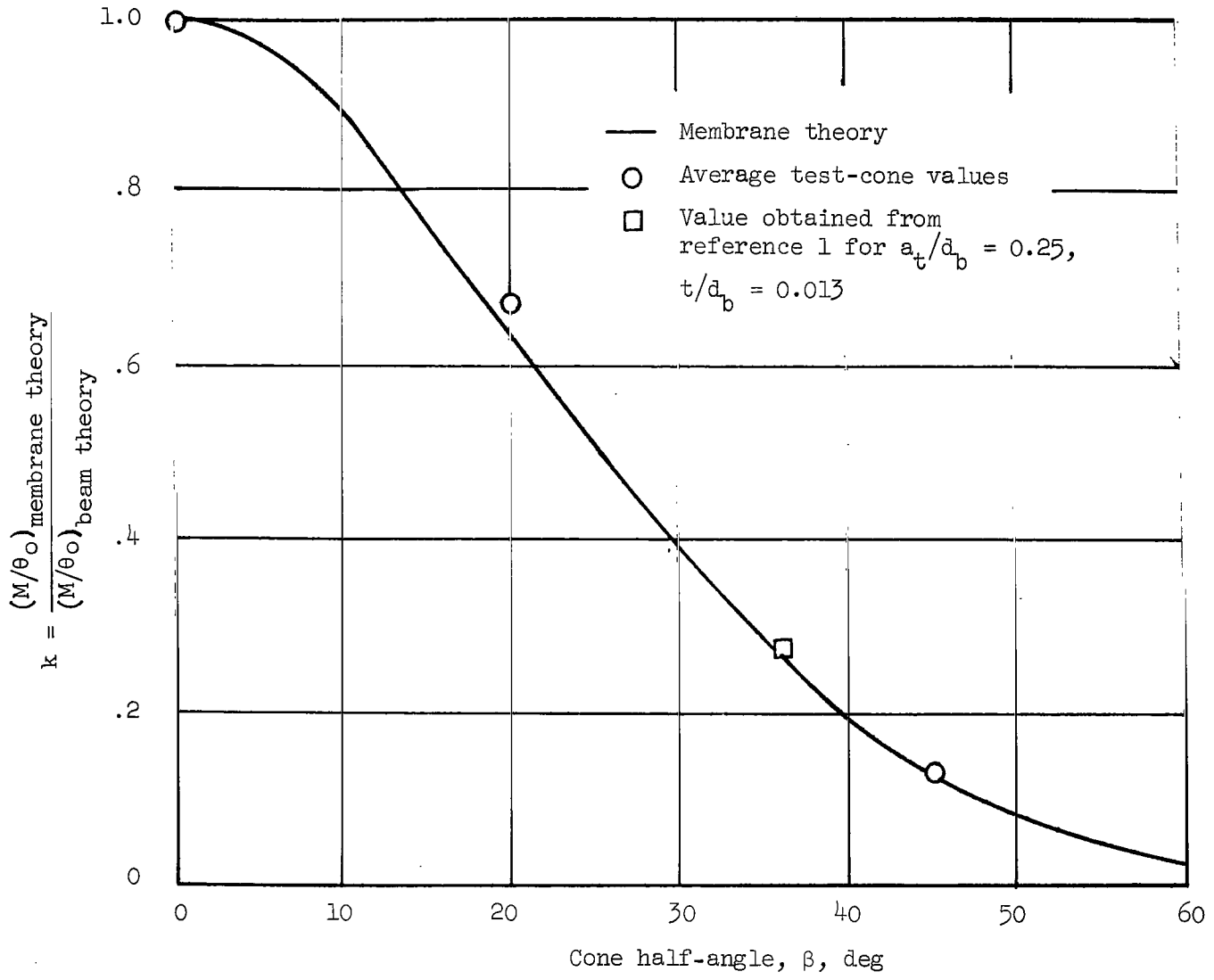

Figure 6.- Variations of correction coefficient k with cone half-angle.

NATIONAL AERONAUTICS AND SPACE ADMINISTRATION
WASHINGTON, D.C. 20546

OFFICIAL BUSINESS

FIRST CLASS MAIL

POSTAGE AND FEES PAID
NATIONAL AERONAUTICS AND
SPACE ADMINISTRATION

"The aeronautical and space activities of the United States shall be conducted so as to contribute . . . to the expansion of human knowledge of phenomena in the atmosphere and space. The Administration shall provide for the widest practicable and appropriate dissemination of information concerning its activities and the results thereof."

—NATIONAL AERONAUTICS AND SPACE ACT OF 1958

NASA SCIENTIFIC AND TECHNICAL PUBLICATIONS

TECHNICAL REPORTS: Scientific and technical information considered important, complete, and a lasting contribution to existing knowledge.

TECHNICAL NOTES: Information less broad in scope but nevertheless of importance as a contribution to existing knowledge.

TECHNICAL MEMORANDUMS: Information receiving limited distribution because of preliminary data, security classification, or other reasons.

CONTRACTOR REPORTS: Scientific and technical information generated under a NASA contract or grant and considered an important contribution to existing knowledge.

TECHNICAL TRANSLATIONS: Information published in a foreign language considered to merit NASA distribution in English.

SPECIAL PUBLICATIONS: Information derived from or of value to NASA activities. Publications include conference proceedings, monographs, data compilations, handbooks, sourcebooks, and special bibliographies.

TECHNOLOGY UTILIZATION PUBLICATIONS: Information on technology used by NASA that may be of particular interest in commercial and other non-aerospace applications. Publications include Tech Briefs, Technology Utilization Reports and Notes, and Technology Surveys.

Details on the availability of these publications may be obtained from:

SCIENTIFIC AND TECHNICAL INFORMATION DIVISION

NATIONAL AERONAUTICS AND SPACE ADMINISTRATION

Washington, D.C. 20546